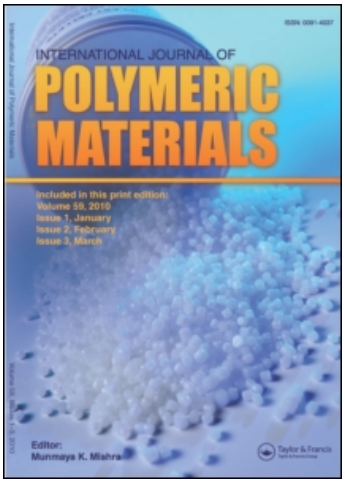

International Journal of Polymeric Materials
Publication details, including instructions for authors and subscription information:
http://www.informaworld.com/smpp/title~content=t713647664

The Role of Matrix in the Compressive Strength of Polyethylene Fiber Composites

Kwang G. Kim[a]
[a] Yukong Limited, Taedok Institute of Technology, Taejon, Korea

To cite this Article Kim, Kwang G.(1998) 'The Role of Matrix in the Compressive Strength of Polyethylene Fiber Composites', International Journal of Polymeric Materials, 39: 3, 173 — 199
To link to this Article: DOI: 10.1080/00914039808039767
URL: http://dx.doi.org/10.1080/00914039808039767

Intern. J. Polymeric Mater., 1998, Vol. 39, pp. 173–199
Reprints available directly from the publisher
Photocopying permitted by license only

The Role of Matrix in the Compressive Strength of Polyethylene Fiber Composites

KWANG G. KIM

Yukong Limited, Taedok Institute of Technology, 140-1 Wonchon-Dong, Yusung-Ku, Taejon, Korea

(Received 20 September 1996; In final form 10 May 1997)

Composites reinforced with polyethylene fibers of Spectra type are noted for low compressive strength. Therefore, they may have limitations in structural applications. The objective of present study was to determine to what an extent the compressive properties are affected by the matrix material. Of proposed theories of composite compressive strength, we found Piggott's theoretical and experimental work most satisfactory especially in the modified form.

Keywords: Compressive strength; polymeric composites; fiber reinforcement; polyethylene fibers; spectra fibers; matrix properties; adhesion

I. INTRODUCTION

A. General Considerations

A satisfactory analysis of compressive strength of fiber reinforced composite remains to be a difficult problem. This situation exists because;

(1) Rigorous analysis of the strength of materials is always difficult, especially for composite materials.
(2) Matrix (or fiber) properties in composites may not be the same as the properties of neat resin (or fiber).
(3) Strength is controlled by the weakest element in the structure whose properties are very difficult to determine.

(4) Quality of specimen depends much on the fabrication procedures, e.g., flow of matrix, misalignments of fibers, internal stresses, voids, etc.

In addition, the compressive properties are more difficult to analyze than tensile properties since;

(5) Compressive and transverse properties of fibers cannot be measured directly.
(6) Young's modulus (or strength) is often much less than the rule of mixture value.
(7) Several modes of failure are possible and the correct mode of failure is difficult to determine even with microscopical analysis.

Properties of composites, especially strength, depend not only on the intrinsic properties of constituent materials and their interfaces but also on composite fabrication techniques, environment effects, and variations in test methods. In this report, the main emphasis is given to the effects of the intrinsic properties of the constituent materials and their interfaces.

B. Review of Theories

Theoretical developments of compressive strength of composites have been slow. Rosen [1] was the first to attempt to explain the compressive strength. His theory was based on elastic buckling of the fibers, and produced a result of the form

$$\sigma_{1u} = E_m/2(1 + \nu_m)(1 - V_f) \tag{1}$$

where σ_{1u}, E_m, V_f, ν_m are the strength of composite in the fiber direction (1-direction), modulus of matrix, fiber volume fraction, and Poisson's ratio of the matrix, respectively. This equation indicates that σ_{1u} increases with V_f but is dominated by the shear modulus of the matrix. Equation (1) has two problems, i) it does not give the correct relation for the variation of the compressive strength with fiber content, ii) it predicts values that are much too great compared to experimental data. The value from equation (1) may represent the theoretical maximum value.

Before this strength can be achieved, other failure modes supervene. For example, Hayashi and Koyama [2] suggested that matrix yielding initiates failure. For continuous fiber composites, this leads to

$$\sigma_{1u} = (V_f E_f + V_m E_m)\varepsilon_{my} \tag{2}$$

where E_f, V_m, ε_{my} represent fiber modulus, matrix volume fraction and matrix yield strain, respectively. This expression gives the required variation of strength with V_f, though the hypothesis that the composite fails at the matrix yield strain does not conform to the experimental results [3].

Since these equations are based on unrealistic assumptions, and the models are too simplified to describe adequately the failure of composite materials, few applications of these equations could be found. Because of these obvious shortcomings, no further discussion will be given to these equations.

Recently, evidences that fibers cannot be assumed to be infinitely strong [4], adhesion breakdown [5], matrix yielding [6], and fiber straightness effect [7, 8] were provided. In addition, fiber bunching, presence of voids, fiber and matrix viscoelastic properties, nonisotropic properties of fibers (Kevlar and carbon fiber) and fiber yielding (Kevlar) are expected to affect the strength of composites. Considering these additional factors, it is likely that there are a great number of possible failure processes, each of which will have its own governing equations. A theory considering some of these phenomena was developed recently by Piggott [9, 10]. In his theory, he considered the failure mechanisms governed by the fibers, the matrices, and the fiber-matrix interfaces. Since Piggot's approaches are the basis for our current theoretical work as well as for our experimental plan, we present below a detailed review of his findings.

C. Piggott's Work

a. Fiber Failure Mode

When the fibers are relatively weak in compression, fiber failure governs composite failure (it is not necessary for the fibers to be weaker than the matrix for this type of failure to occur). This is the case with

Kevlar, which gives composites with quite low compressive strengths and moduli: Kevlar pultrusions fail when the fibre's stress has reached about 0.28 GPa [6]: compare this with Kevlar's tensile strength of 3.5 GPa.

It was found that resins reinforced with aligned steel fibres obeyed the modified rule of mixture

$$\sigma_{1u} = V_f \sigma_{fu} + V_m E_m \sigma_{fu}/E_f \tag{3}$$

where σ_{fu} is the fiber compressive strength. This expression was obeyed over the range tested: V_f from 0.15 to 0.34 and σ_{fu} from 1.3 to 2.26 GPa [2, 8].

With the very straight fibers used in these experiments, matrix support appeared to prevent the fiber buckling when they yielded, giving σ_{fu} values about 80% above the fiber yield stress.

In the case of glass fiber-reinforced-plastics, carbon fiber composites, and boron composites, compressive strength were not governed by this equation [9].

b. Matrix Yielding Mode

It is reported that composite strength depends on the degree of fiber curvature [8, 11]. In this situation, as stress increases, matrix will be pushed aside by the curved fiber, and the stress by the curved fiber approaches the matrix yield stress, σ_{my}. At the onset of this unstable state, the composite begin to yield and fiber compressive stress reaches the maximum value, $\sigma_{f\max}$. We assume in this case that the fibers adhere perfectly to the matrix until failure.

The composite strength in this mechanism is expressed by:

$$\sigma_{lu} = \sigma_{f\max}(V_f + V_m E_m/E_f) \tag{4}$$

This assumes that the matrix is still elastic, which is normally the case [10]. We also have the following relationship from the analysis of fiber geometry [10, 12]

$$\sigma_{f\max} = 2\lambda^2 \sigma_{my}/a\pi^3 = (8R/\pi d)\sigma_{my} \tag{5}$$

where λ, and "a" are the wavelength and amplitude of the curved fibers. If it is assumed that the wave of fiber can be represented by sine wave function $y =$ a sin (x/λ) and R is the radius of curvature, then equation (4) can be expressed as

$$\sigma_{1u} = (2\lambda^2/a\pi^3)(V_f + V_m E_m/E_f)\sigma_{my}$$

$$= (8R/\pi d)(V_f + V_m E_m/E_f)\sigma_{my} \tag{6}$$

This is the strength of composites for the fiber-buckling-matrix-yielding mode of failure. A few supports for this failure mechanism can be found in recent reports [13, 14]. Of particular concern are values of R and d extracted by curve fitting which seem to be unrealistic and cannot be determined by an independent method. A verification of Eq. (6) is therefore still missing and its merits uncertain.

c. Interface and Matrix Tensile Failure Mode [10]

When the interface is weak, the stress can cause separation between the fiber and the matrix. This can be followed by matrix splitting as illustrated in Figure 1. In the figure, compressive stress is applied on the plane of the page and the fibers are aligned perpendicular to the plane of the page, σ_a is adhesion strength between fiber and matrix, and σ_{mtu} the tensile strength of the matrix. When we take into account the relative areas over which these stresses act, we get an approximate equilibrium of forces (9),

$$P = \pi\sigma_a + (\sqrt{P_f}/V_f - 2)\sigma_{mtu} \tag{7}$$

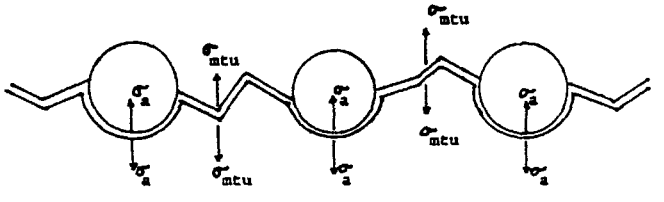

FIGURE 1 Interface and matrix failure, showing stresses involved.

The assumptions here are that once debonding and cracking have taken place, the composite is weakened and that σ_a is the same in all directions but operates throughout the whole area of the fiber, $\pi d/2$, per unit length. P_f is a factor representing the fiber packing arrangement, and is equal to $2\pi/\sqrt{3}$ for hexagonal packing, and π for square packing.

At the onset of failure, the compressive strength of composite is given by

$$\sigma_{1u} = (4R/\pi d)(\pi\sigma_a + (\sqrt{P_f}/V_f - 2)\sigma_{mtu})(V_f + V_m E_m/E_f) \qquad (8)$$

This equation may be used to account for the anomalous volume fraction effects observed with poorly adhering interfaces by Hancox [5] and Martinez *et al.* [8]. For low volume fractions, where σ_{1u} increases linearly with V_f, we use equation (6). At higher volume fractions, where the linear relation between σ_{1u} and V_f no longer holds, we use equation (8). However, it has been noted that while equation (8) predicts the trends correctly the actual values are not so well predicted. This could well be because of extraneous factors, such as poor wet-out with the high V_f poor adhesion samples, leading to very low effective values of σ_{mtu}.

We continue with additional explanations and applications of equations (6) and (8) in the following. Figure 2 shows the effect of matrix yield stress on the failure modes of composites. If matrix is soft relative to fiber, equation (6) will govern and so $\sigma_{1u} \propto \sigma_{my}$. This was indeed the case as shown in Figure 2 with glass fiber reinforced soft polyesters for σ_{my} ranging from about 0.3 to 60 MPa for $V_f = 0.31$.

The equation $\sigma_{1u} = 9\sigma_{my}$ describes the results over this very large range of values of σ_{my} with great fidelity. Above 60 MPa, the strength doesn't change significantly and it is therefore very likely that a different failure process takes over. As indicated previously, we expect the failure of Kevlar composites to be controlled by fiber compressive failure. However, if we use soft enough matrices, we would expect the fibers to be able to push the matrix aside, for all values of $\sigma_{f\max} < \sigma_{fu}$. The Kevlar results fit equation $\sigma_{1u} = 9\sigma_{my}$ in the range 0.3 to 10 MPa as shown in Figure 2, and the fiber failure mode followed with σ_{my} in the range of 10 to 80 MPa.

The combined effects of adhesion and fiber volume fraction are shown in Figure 3. The curves for transverse composite failure were

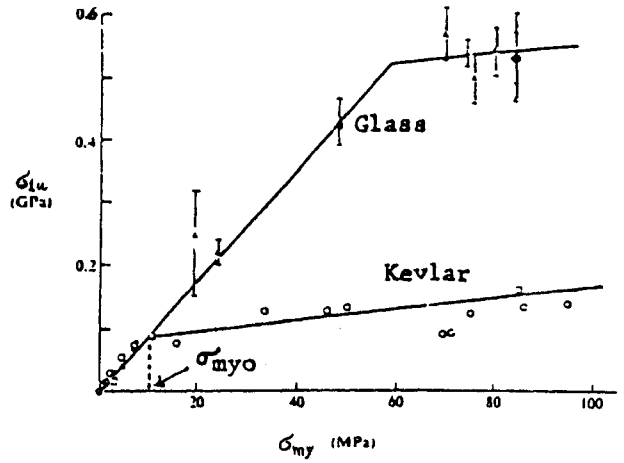

FIGURE 2 Composite strength against polyester matrix yield strength. (For clarity the error bars have been omitted for the glass composites with $\sigma_{my} < 10$ MPa. For the Kevlar composites the standard deviations are normally less than the radii of the circles indicating the results (6).

plotted using equation (6) and for splitting failure using equation (8) 50% adhesion means that $\sigma_a/\sigma_{mtu} = 0.5$. For perfect adhesion we replace $\pi\sigma_a$ by $2\sigma_{mtu}$ (it is expected that the matrix under the fiber, rather than the interface, fails in this case). For example, consider a polymer matrix which is 50% stronger in compression than in tension, i.e., $\sigma_{mcu} = 1.5\ \sigma_{mtu}$. Since the mechanism which is activated at the lowest stress prevails, it is expected that the failure will be governed by the "transverse compression" with V_f in the range of 0 to 0.4. Above $V_f = 0.4$, splitting failure is predicted. This type of plot with $\sigma_{mcu}/\sigma_{mtu} = 1.5$ can be made to fit the results of Martinez *et al.* [8] as shown in Figure 4. The results observed by Hancox [5] with carbon fiber epoxy composites may also be explained by this combination of failure processes.

Figure 4 shows a good fit to the experimental results using equation (6) with $\sigma_{my} = 130$ MPa for the linear region near the origin, and equation (8) for higher values of V_f with $\sigma_{mtu} = 33$ MPa.

Also, various values of σ_a indicated on the figure for the rest of the results. Note that plot indicates a perfect adhesion (i.e., $\sigma_a = \sigma_{mtu}$) for the fibers with the sizing agent removed.

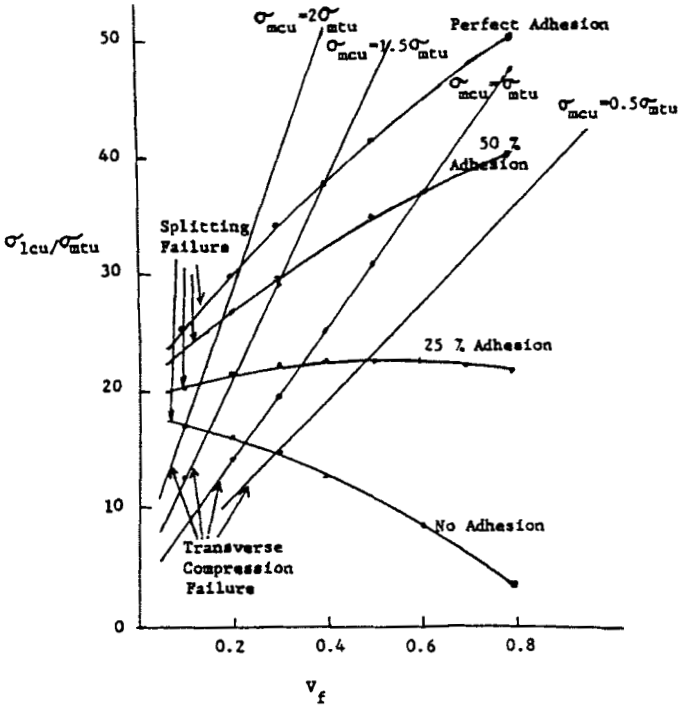

FIGURE 3 Dimensionless plot for composite compressive strength when controlled by transverse splitting and transverse matrix compression failure.

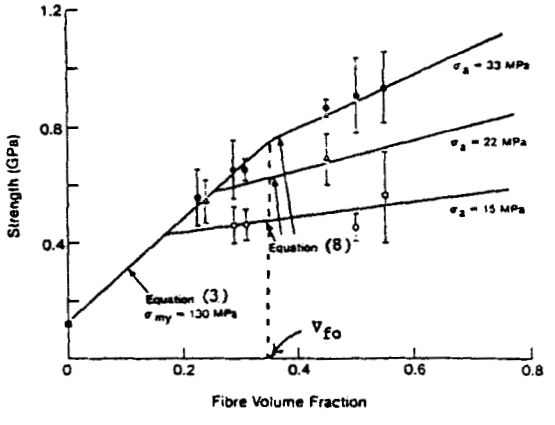

FIGURE 4 Fitting poor adhesion results for glass pultrusions by use of equation (6) and (8). The solid circles are as-received fibers (sizing intact), triangles are solvent soaked fibers, and the open circles are fibers which have had their sizing removed by heat (8).

II. FACTORS AFFECTING THE COMPRESSIVE STRENGTHS OF COMPOSITES

A. Compressive Properties of Fibers

Organic fibers have been originally developed for use in tension and low bending rigidity. Only recently, aramids penetrated the area of high performance composites. The progress was rather slow because of the relatively low compressive strength that was the subject of numerous articles in the technical literature. Nevertheless, the progress was steady and aramids have now an important place in the technology of high performance composites. In areas where high compressive strength is required, the problem has been effectively overcome by hybridization.

Spectra-900 fibers are thermoplastic and therefore, strain rate sensitive, which could represent an additional limitation beyond the expected low compressive strength. As it will be shown below, we expect the compressive strength of Spectra-900 to be below that of glass and carbon fibers, but not necessarily below that of aramid fibers. At present we do not have any data on compressive strengths of Spectra-900 fibers. The composite research is still in its early stages and the available data do not allow meaningful estimates of these vital fiber properties. In cases where compressive properties of composites depend on fiber compressive strengths, the results usually fall below the specifications based on aramid fibers. However, the causes for this deficiency could be several and at this stage, we cannot yet conclude what is the major problem.

In this section, we present a brief review of compressive properties of thermoplastics as well as aramid fibers with the objective to establish preliminary targets for the properties of Spectra-900 fiber composites.

The compressive properties of PET and nylon 6 were determined in our laboratories [15]. The measurements were made on rather thick filaments 0.025″ diameter which were cut to make a short cylindrical sample with the length to diameter ratio of approximately 3.0. These samples were then placed in a holder consisting of a brass block about 1″ high having a vertical hole drilled in it just large enough for a sample to loosely fit into it. A steel rod, also a loose fit in the hole and lubricated with graphite, rested on the sample and transmitted the force from the compression cell of an Instron testing machine.

These results showed that for moderately oriented fibers, the ratio of moduli is approximately:

$$\frac{E\,(\text{compression})}{E\ (\text{tension})} = 0.7$$

This ratio was observed both with PET fibers whose compression modulus was 1.16 GPa and nylon 6 fibers whose E(comp) was only 0.3 GPA. The compressive yield strains were, with both fibers, in the range of 3–4% and, therefore, the yield stresses of 0.04 GPa and 0.01 GPa are obtained, respectively. Common PET and nylon 6 monofilaments have, therefore, very low compressive strength which is reflected in their bending recovery behaviour. There are no reliable data on composites to verify these findings.

Kevlar fibers, on the other hand, exhibit considerably higher compressive strength compared to organic low modulus fibers, as established on pultrusion type composites (6).

$$\sigma_c\,(\text{Kevlar}) = 0.28\ \text{GPa} = 4.1 \times 10^4\ \text{Psi}$$

Failure of fibers in compression is similar to that of metals. Kink bands are formed along the preferred crystallographic slip planes. While it is possible to estimate the energies involved in such processes, the calculations must also include morphological data on fibers. These are not sufficiently known to make such analyses worthwhile.

A much simpler approach is to consider the average cohesive energy densities of the systems, neglecting the morphological details, and assuming that compressive strength is proportional to the cohesive energy density of the system. Since fiber failure is along the crystallographic slip planes, not 3-dimensional, the comparison should be based on the aerial cohesive energy densities as shown in Table I.

The cohesive energy of polyethylene is well known and amounts to

$$\left(\frac{E_{\text{coh}}}{V}\right)_{PE} = 72.3\ \text{cal/cc}$$

TABLE I

	PE[1]	*PTP*[2]	*PVA*[2,3]
(E_{coh}/V), cal/cm^3	72.25	159	204
$(E_{coh}/V)^{2/3}$	17.4	24.4	34.7
(density)$^{2/3}$	0.97	1.54	1.22
$(E_{coh}/V)^{2/3}$(density)$^{2/3}$ (SACED), (cal/gr)$^{2/3}$	18.0	19.1	28.5

1. Values are from experiments.
2. From the estimation by group contribution procedure [16].
3. Listed for comparison.

Group contributions using Van Krevelen's table (16) yield for polyphenylene terephthalamide (PTP, Kevlar®)

$$\left(\frac{E_{coh}}{V}\right)_{PTP} = 159.0 \text{ cal/cc}$$

These values yield the following specific aerial cohesive energy densities (SACED) along the fracture planes

$$(\text{SACED})_{PE} = 18.0 \text{ (cal/gr)}^{2/3}$$

$$(\text{SACED})_{PTP} = 19.1 \text{ (cal/gr)}^{2/3}$$

In comparing these values it must be recognized that the SACED of PE is based on experimental data of the cohesive energy density (E_{coh}/V) as well as realistic densities. With PTP and PVA on the other hand, we used a group contribution procedure based on the data from small molecules [16] to estimate (E_{coh}/V). This computation yielded 159 cal/cm^3 and 204 cal/cm^3, respectively.

Since the realistic density of PTP is 1.54, we first made a very conservative estimate of the SACED using the estimated cohesive energy density and crystalline density of PTP. This approximately yielded

$$(\text{SACED})_{PTP} = 22.1 \text{ (cal/gr)}^{2/3}$$

which must be considered as the upper bound for $(\text{SACED})_{PTP}$.

A more proper estimate can be obtained by using estimated density of PTP using group contribution tables as in the case of cohesive

energy density $\rho_{\text{calc. PTP}} = 1.92$ (gr/cm^3). This value yields

$$(\text{SACED})_{\text{PTP}} = 19.1 \text{ (cal/gr)}^{2/3}$$

which is in our opinion the most relevant estimate we can obtain without going into more complicated calculation involving adjustments in (E_{coh}/V) due to lower density of polymers than of small molecules using the Leonard-Jones potentials.

In comparing the compressive properties of PE and PTP, microstructures of extended chain PE and PTP fibers must not be overlooked. Both fibers fibrilate relatively easily, which reflects poor transverse properties. But splitting of PTP can be accomplished more readily than PE. To some extent this could be attributed to the epitaxial crystallization of PE, a phenomenon frequently observed in heat sealing of PE. Since the epitaxial crystallization of PE should occur also on the microstructural level (i.e., between the microfibrils), we believe that extended chain PE could be prepared more easily than PTP with enhanced transverse properties. Therefore, we anticipate that ultimately we will be able to produce PE fibers with the specific compressive strength exceeding that of Kevlar fibers.

On the basis of these approximations, we should expect that the specific compressive strength of PE and Kevlar reinforced composites should be sbout the same. If PVA is considered briefly, this material shows on the basis of SACED consideration (see Tab. I) about 50% higher specific compressive strength than Kevlar. Considering in addition much stronger adhesive bonding to expoies, an ultrastrong PVA could be a highly effective reinforcing material for composites.

Finally, we want to point out that these estimates should serve only as a guideline to establish the range where these properties should fall and that the compressive strength of composites should also depend on matrix selection, fabrication methods of composites as well as the morphological characteristics of the fibers.

B. Expansion and Revision of Piggott's Theory: Compressive Properties of Net Resins and Matrix Selection Guides

We understand from the previous works (8, 11) that compressive properties of neat resins have the following generalizations;

i) Curing increases both yield stress and strain, and increases the level of stress at all strains.
ii) In a given resin system, high modulus material has high yield stress, and this is true for both partly cured and fully cured systems.
iii) The apparent compressive strength (σ_{mu}), when it exists, is also approximately proportional to yield stress for fully cured resins.

To understand more about resin properties, we reviewed tensile and compressive properties of commercially available resin's [17–21]. Table II shows some of the data and Figure 5 illustrates the tensile strength and compressive yield stress of the resins from Table II.

In Table II, we see that each property varies in a wide range, and there is no apparent correlation between σ_{my} and σ_{mtu} as we see in Figure 5. In many high strength resins, the curing temperatures are not acceptable for spectra-900 composites, since the fibers will melt at about 140°C. For such resins to be used in composite fabrication, we should modify the curing system or conditions (curing agent or curing time), so that curing below 120°C can yield the desired high resin properties.

Another factor to note in Table II is the strains applied at failure or yielding. Some of the high compressive yield stress resins show yield strains about 50%, which are not acceptable for structural applications. Previously, modulus served as a criterion of the matrix was thought to be the single most important parameter for better compressive strength of composites from the understanding of Rosens's equation and the generalizations previously mentioned. However, this cannot be accepted without consideration of strains involved in the failure processes.

The importance of strain factor in composite failure can be considered by rewriting equations (3), (6) and (8) as follows:

$$\begin{aligned}\sigma_{1u} &= \sigma_{fu}V_f + \sigma_{fu}V_m E_m/E_f \\ &= (E_f V_f + E_m V_m)\varepsilon_{fu} \end{aligned} \tag{9}$$

$$\begin{aligned}\sigma_{1u} &= \sigma_{\mathrm{fmax}}(V_f + V_m E_m/E_f) \\ &= (8R/\pi d)(V_f + V_m E_m/E_f)\varepsilon_{my} \\ &= (8R/\pi d)(V_f + V_m E_m/E_f)(E_m \varepsilon_{my}) \end{aligned} \tag{10}$$

TABLE II Collection of epoxy resins showing different grades of mechanical properties

		σ_{mtu}					
Grade		*High*		*Medium*		*Low*	
Sample Designation		*1*	*2*	*3*	*4*	*5*	*6*
Resin System		*ERLA 2256 Epoxy*	*Epon 828 /Z, 20 phr*	*MY720/ HT976 44 phr*	*30 DER 736, 70 DER 331/ 3 BF_3 MEA*	*DER 331/ BF_3 MEA, 3 phr*	*70 Araldite 6005/ 30 Lancast A*
Tensile	E	545	360	540	454	402	130
Property	σ_y		8.0				
	ε_y		2.2				
	σ_u	14.0	13.0	8.54	8.93	4.17	3.6
	ε_u	4.0	4.8	1.8	6.45	1.1	
Compressive	E		460	280	264	261	230
Property	σ_y		10.5	29.0	40.5	16.9	7.6
	ε_y		2.6		50.0		5.0
	σ_u	29.0	19.0	34.0	40.5	31.3	19.9
	ε_u		8.7		50.0	34.8	61.4
Reference		19	20	22	21	21	22

TABLE II (Continued.)

		σ_{my}					
Grade		*High*		*Medium*		*Low*	
Sample Designation		7	8	9	10	11	12
Resin System		*30 DER 732, 70 DER 331/ 23 MDA*	*30 DER 736, 70 DER 331/ 3 BF_3 MEA*	*30 DER 736 70 DER 331/ 350–400 AHEW Polymide*	*100 DER 331, 87.5 NMA 1.5 BDMA*	*EPON 828/ AEP, 20phr*	*75 Araldite 502/3 DY064, 25 Lancast A*
Tensile Property	E	392	454	242	430	400	170
	σ_y					5.0	
	ε_y					1.4	
	σ_u	8.95	8.93	4.83	8.48	9.6	3.8
	ε_u	6.8	6.45	15.3	2.2	8.8	
Compressive Property	E	316	264	174	287	380	200
	σ_y	38.2	40.5	26.7	18.7	8.7	5.8
	ε_y	49.8	50.0	53.5	12.0	3.5	4.7
	σ_u	38.2	40.5	26.7	37.1	13.8	20.3
	ε_u	49.8	50.0	53.5	52.3	10.5	57.3
Reference		21	21	22	21	20	22

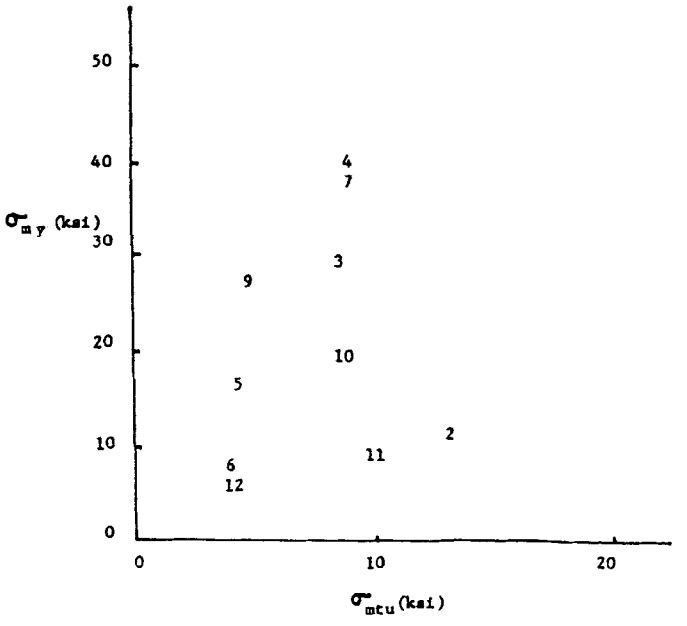

FIGURE 5 Collection of resin data, tensile strength (σ_{mtu}) and compressive yield stress (σ_{my}).

$$\sigma_{1u} = (4R/\pi d)(\pi\sigma_a + (\sqrt{P_f}/V_f - 2)\sigma_{mtu})(V_f + V_m E_m/E_f)$$

$$= (4R/\pi d)(\pi E_a \varepsilon_{au} + (\sqrt{P_f}/V_f - 2)E_m \varepsilon_{mtu})(V_f + V_m E_m/E_f)$$

$$= (4R/\pi d)(\pi E_a + (\sqrt{P_f}/V_f - 2)E_m)(V_f + V_m E_m/E_f)\varepsilon_{mtu} \qquad (11)$$

In equation (11), the ultimate strain of the interface region, ε_{au}, was assumed to be equal to ε_{mtu} to emphasize the role of strain.

In fiber controlled failure, the fibers fail before matrix or interface failure takes place. Therefore, in equation (9), the composite failure strain will not exceed fiber ultimate strain which is usually less than 3 to 4% as considered in Section A. Therefore, most matrices would be elastic until composite fails and matrix selection would not be difficult if this mechanism governs. However, in the matrix yielding mechanism equation (10), composites will fail at the matrix compressive yield

strain. In the interface and matrix tensile splitting failure mechanism, equation (11), composites will fail at the ultimate tensile strain of the matrix.

To summarize, in most structural composite applications, where V_f is usually high, these resins which have high values of σ_a and σ_{mtu}, not σ_{my}, will be the primary candidates, since the interface and matrix tensile failure will be the governing mechanism. Since large strains cannot be allowed for structural applications, the modulus has to be high also.

The equations in the previous chapter can be used in determining important parameters in the selection of matrices by obtaining derivatives of each equation with respect to each variable. By introducing the value of each variable into those derived equations, we could get the approximate range of strength changes with respect to the variation of each variable. Table III shows the assumed range of each variable, and Table IV shows the approximate values of the derivatives obtained in this manner.

From Table IV, we can find the relative importance of each parameter in each mode of failure. For the fiber failure mode, we see the change of V_f will give the most significant effect, and next σ_{fu}. For the fiber-buckling-matrix-yielding mechanism, the importance will be given in the order of $\sigma_{my} > V_f > R/d > E_m$. For interface and matrix tensile failure mode the order of importance is $\sigma_a > \sigma_{mtu}$, $V_f > R/d > E_m$. Therefore we can select matrices on the basis of σ_{my} in the case of low fiber content composites, where equation (6) governs. When fiber content is high where equation (8) governs, σ_{mtu} is expected to serve as a criterion, since σ_a is expected to be obtained up to perfect adhesion by surface treatment of the fibers. These orders of importance of parameters could be used when we select matrix parameters to optimize composite performances, and this shows the resin properties could largely determine the compressive strength of composites. On

TABLE III Assumed ranges of variables

Fiber	*Matrix*	*Miscellaneous*
$V_f = 0.1$ to 0.8	$E_m = 0.7$ to 14.0 GPa	$R/d = 11.0$
$E_f = 100$ to 130 GPa	$\sigma_{my} = 0.1$ to 0.35 GPa	$P_f = 3.14$ to 3.63
$\sigma_{fu} = 2.0$ to 5.0 GPa	$\sigma_{mtu} = 0.02$ to 0.10 GPa	$\sigma_a = 0.01$ to 0.1 GPa

TABLE IV Equations of the range of derivatives using values given in Table III

i) From Equation (3)

$(\partial\sigma_{1u}/\partial E_m) = 0.002 \sim 0.035$
$(\partial\sigma_{1u}/\partial\sigma_{fu}) = 0.10 \sim 0.91$
$(\partial\sigma_{1u}/\partial V_f) = 1.72 \sim 4.97$
$(\partial\sigma_{1u}/\partial E_f) = \sim 0.001$

ii) From Equation (6)

$(\partial\sigma_{1u}/\partial(R/d) = 0.03 \sim 0.74$
$(\partial\sigma_{1u}/\partial\sigma_{my}) = 2.9 \sim 23.2$
$(\partial\sigma_{1u}/\partial V_f) = 2.8 \sim 8.4$
$(\partial\sigma_{1u}/\partial E_m) = 0.004 \sim 0.08$

iii) From Equation (8)

$(\partial\sigma_{1u}/\partial(R/d) = 0.03 \sim 0.2$
$(\partial\sigma_{1u}/\partial\sigma_a) = 4.6 \sim 35.8$
$(\partial\sigma_{1u}/\partial\sigma_{mtu}) = 0.7 \sim 9.3$
$(\partial\sigma_{1u}/\partial V_f) = 1.0 \sim 5.9$
$(\partial\sigma_{1u}/\partial E_m) = 0 \sim 0.03$

this account, σ_{my} and σ_{mtu} were used as a selection criterion of different resins in Table II.

Finally, chemical structures of these selected resins were considered for the understanding of the structure-property relations. Table V shows chemical structures of those resins with different grades of tensile strengths and compressive yield stresses. The properties of cured epoxy resins depend on the structures of both resin and curing agent. Generally, aromatic curing agents give better rigidity and strength to the heat distortion temperature, brittleness. and chemical resistance (22). However, in Table V, the highest values of σ_{my} and σ_{mtu} are coming from bis-phenol-A type, cycloaliphatic or aliphatic epoxy resins, not from epoxy-nonvolac type resins. These high strengths may be from the higher strains applicable to these more flexible molecular chains. Also, we see in Table II that mixing of two different resins could yield high strengths, and therefore could be tried in our future experiments.

III. EXPERIMENTAL FRAMEWORK

For experimental purposes, the equations in Chapter I were modified, since the original equations included some uncertain variables such as

TABLE V Chemical structures of resins

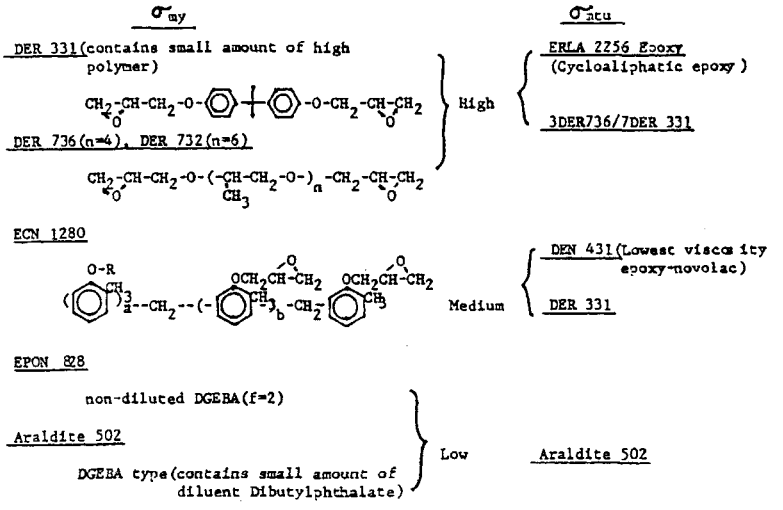

σ_{fu}, $\sigma_{f\max}$, and R/d. Therefore, Equations (3), (6) and (8) were improved by introducing K, K_1, K_2, K_3 to include of or represent uncertain factors from geometry or structure such as voids, misalignments, cracks, shrinkage, and (R/d). In this sense, K's could be used as a measure of the quality of the samples. Since it is expected that when V_f changes K values also change, σ_{1u} in these equations was expressed as a function of variables other than V_f such as E_m, σ_{my}, σ_{mtu}. Equations rearranged for this purpose are shown in Table VI.

A. Determination of Failure Modes

Failure of fiber composites could happen by the yielding of fiber or matrix if the interface is strong. Therefore, when we plot σ_{1u} vs. σ_{my} we would have a curve like Figure 2. At low σ_{my}, equation (6) will govern, and at high σ_{my}, equation (3) will govern. In this kind of plot, if we increase V_f gradually, the crossover point (σ_{my} in Fig. 2) is expected to move toward the lower values of σ_{my} and σ_{1u} direction.

If we plot σ_{1u} vs V_f at a constant matrix yield stress, the curve will look like Figure 4. At lower V_f, equation (6) will govern, and at higher V_f, equation (8) will govern. As σ_a increases by the surface treatment of fibers, the curve governed by equation (8) will move upward in the

TABLE VI Modifying equations

i) Fiber failure mode (Eq. (3))

$$\sigma_{1u} = K\sigma_{fu}(V_m/E_f)E_m + K\sigma_{fu}V_f \tag{12}$$

ii) Fiber-buckling-matrix-yielding mode (Eq. (6))

$$\sigma_{1u} = K_1(V_m\sigma_{f\max}/E_f)E_m + K_1V_f\sigma_{f\max} = K_2(V_f + V_mE_m/E_f)\sigma_{my} \tag{13}$$

iii) Interface and matrix tensile failure mode (Eq. (8))

$$\sigma_{1u} = K_3(\sqrt{P_f}/V_f - 2)((1 - E_m/E_f)V_f + E_m/E_f)\sigma_{mtu} + K_3(\pi\sigma_a)((1 - E_mE_f)V_f + E_m/E_f) \tag{14}$$

regions of high V_f. If we conduct similar experiments with matrix materials of higher σ_{my}, the crossover point (V_{fo} in Fig. 4.) is expected to move upward the lower σ_{1u} and higher V_f direction.

From this information, we can determine the modes of failure for a composite with a given set of V_f, σ_{my}, and we could also predict the strength of a composite if the necessary data are supplied. In doing these, we assumed that the fiber properties are constant in all cases.

B. Determination of the Hard-to-Obtain Variables

a. Determination of $K\sigma_{fu}$

By plotting σ_{1u} vs. Em (equation (12)), all samples with the condition of $\sigma_{my} > \sigma_{myo}$ and low V_f will yield curves similar to Figure 6. We could get $K\sigma_{fu}$ from the slope or intercept. K and σ_{fu} appear always in a combined form and inseparable, however, we can observe the change of each parameter (K or σ_{fu}) by the effect of ambient temperature or any structural changes as V_f on composite strength. Since we expect that temperature change will cause changes in σ_{fu} of Spectra-900 fiber, not K, and structural changes will cause changes in K, not σ_{fu}, the functional relations can easily be understood from equation (12) (See Tab. VIII also). Since we can measure the composite strengths and obtain the values of all the other variables in equation (12) at different temperatures or fiber contents, we could obtain the ratio of the change of σ_{fu} or K using equation (12). Therefore, if we change ambient temperature at constant V_f, we will obtain the change of σ_{fu} and if we change V_f at constant temperature, the

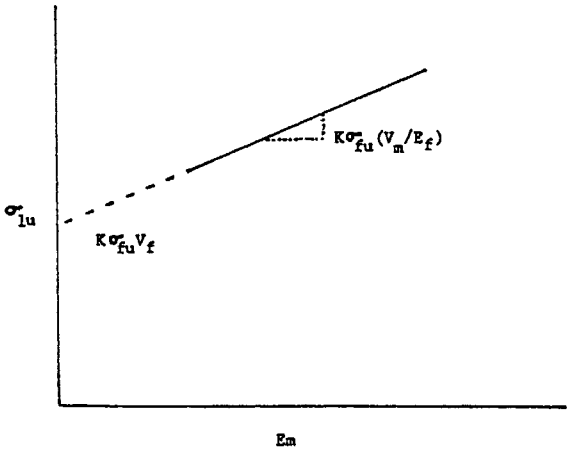

FIGURE 6 A plot to obtain $K\sigma_{fu}$.

effects on σ_{1u} appear in K. From these considerations, we could obtain some information about the influence of temperature or other structural changes to σ_{fu} or K.

b. Determination of K_2

When $\sigma_{my} < \sigma_{myo}$ and $V_f < V_{fo}$, the failure mode will be governed by the fiber-buckling-matrix-yielding mechanism. Therefore, if we plot σ_{1u} vs. σ_{my} under the above conditions, the slope of the curve will give K_2 from equation (13) since the values of all other parameters are known or obtainable (Fig. 7). In this case, we can say that the higher the K_2 value, the better the quality of the composite sample.

c. Determination of P_f

P_f value is determined by the distances(s) between the fibers in the composites. The relations between V_f and s are as follows when the fibers are regularly spaced [23].

$$s = 2r((\pi/2\sqrt{3}V_f)^{1/2} - 1) \qquad \text{(hexagonal arrangement)}$$

$$s = 2r((\pi/4V_f)^{1/2} - 1) \qquad \text{(square arrangement)}$$

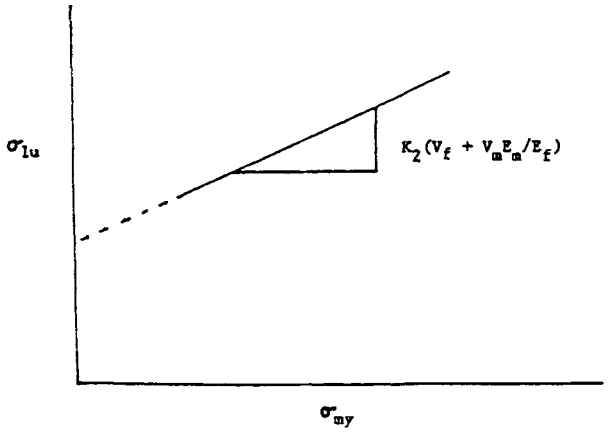

FIGURE 7 A plot to obtain K_2.

By rearranging, both equation yield the following relation.

$$P_f = V_f(s/r + 2)^2 \tag{15}$$

where $P_f = 2\pi/\sqrt{3}$ for hexagonal and π for square arrangements. From Equation (15), we see that if we get s for a given value of V_f and r, we can have P_f or vice versa. Since the distance between fibers in heaxagonal and square arrangements are the two extreme distances which we can get by arranging any number of fibers, we expect average distances between fibers in a randomly arranged sample will fall between these two extreme values (Fig. 8). By measuring the distances between fibers from microscopic picture and averaging them, we can get P_f values from equation (15).

d. Determination of K_3 and σ_a

These parameters appear in equation (14) where interface and matrix tensile failure mechanism governs and can be applied when $\sigma_{my} < \sigma_{myo}$ and $V_f > V_{fo}$. In equation (8) σ_{1u} is nonlinear with respect to V_f, therefore we can choose σ_{mtu} as an independent variable to obtain a linear function (equation (14)). Since we could obtain P_f for any samples, by plotting σ_{1u} vs σ_{mtu}, we can get K_3 from the slope and σ_a value from the intercept. (Fig. 9).

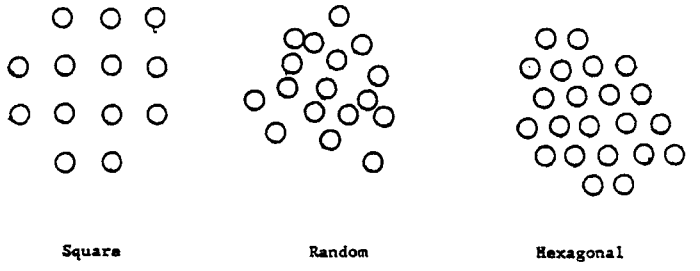

FIGURE 8 Arrangement of fibers in a cross-section of a composite.

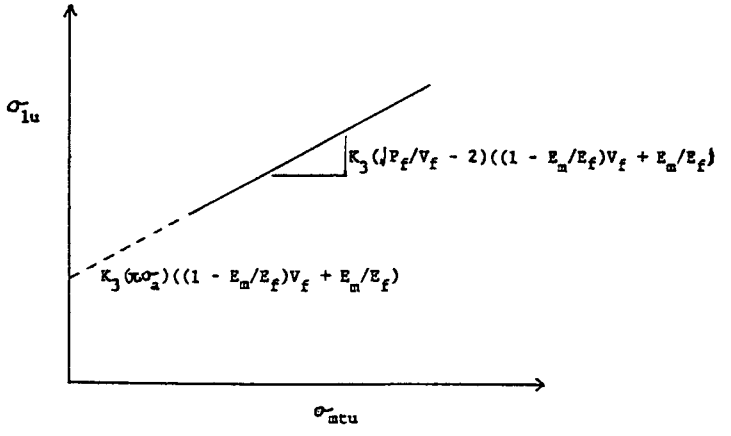

FIGURE 9 A plot to obtain K_3 and σ_a values.

e. Determination of σ_{ft} (Fiber Transverse Strength)

Since it is expected that the transverse properties of Spectra-900 fibers are weak, we could imagine a mechanism where the composites fail by fiber transverse failure and matrix tensile failure as illustrated in Figure 10. If this is the case, we could obtain σ_{ft} by modifying equation (8), replacing $\pi\sigma_a$ with $2\pi\sigma_{ft}$ as shown in equation (16).

$$\sigma_{1u} = K_3(2\pi\sigma_{ft} + (\sqrt{P_f}/V_f - 2)\sigma_{mtu})(V_f + V_m E_m/E_f) \qquad (16)$$

If σ_a is equal to or larger than σ_{ft}, this mode of failure (fiber transverse and matrix tensile failure mode) is expected to occur and equation (16)

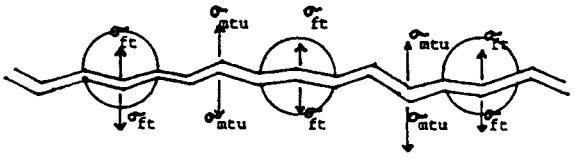

FIGURE 10 Stresses involved in fiber transverse and matrix tensile failure.

can be used. Therefore, by changing the adhesion strength σ_a gradually from low to high (e.g., by treatment of fiber surface with gradual increase of corona discharge dosage), we can expect at certain adhesion strength, the intercept of the curve in Figure 11 will no longer increase, since fibers split instead of interface failure, then we can assume at this point that σ_{ft} is equal to σ_a.

One of the purposes here is to get the highest values of $K\sigma_{fu}$, K_2, K_3 by optimizing various properties of the matrix materials and fabrication methods, and high values of these parameters mean high quality of the composite specimens. Another purpose here is to obtain the hard-to-obtain parameters as described above.

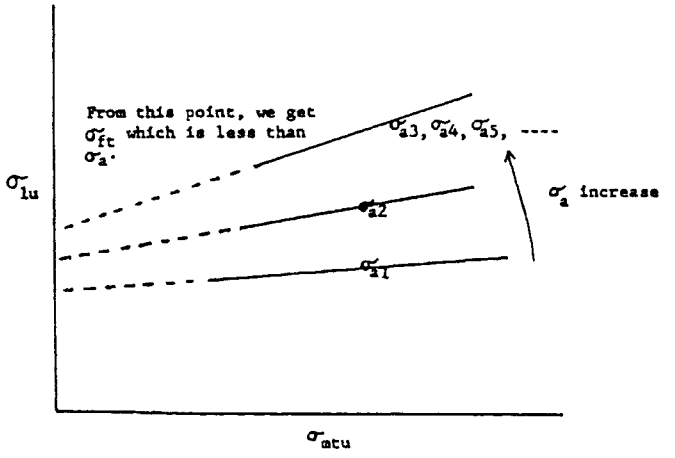

FIGURE 11 Experimental scheme of obtain fiber transverse strength, σ_{ft}. In the figure, $\sigma_{a1} < \sigma_{a2} < \sigma_{a3} < \sigma_{a4} < \sigma_{a5}$-----.

C. Effects of Strain Rate and Temperature

In structural applications of composite materials, the influence of environmental effects and strain or stress rate should be considered. Particularly, in Spectra-900 composites, the strain rate and ambient temperature are expected to affect their performance significantly, since fiber itself is thermoplastic. The effects of strain rate and ambient temperature on the properties of Spectra-900 fiber, some of the chosen matrix materials, and one glass-fiber-polyester pultrusion are summarized in Table VII. We see that the fiber, matrix material, and composite, are all affected significantly by temperature and strain rate.

TABLE VII Strain rate and temperature effect on the properties of Spectra-900 fiber, matrix materials, and composite

i) Spectra-900 fiber
Creep at 1/10 of its breaking load (3gr/denier)
at room temperature; 2.5%/600hrs
at 160°F; 70%/30 hrs

ii) Matrix materials
Strain rate effect (9)

Speed (mm/min)	*Resin (Polyester)*	
	Yield Strength (MPa)	*Modulus (GPa)*
0.05	74	3.3
0.5	94	3.3
5.0	96	3.6
50.0	117	3.7

Temperature effect (Epon 828/Z)

Temp (°C)	*25*	*50*	*75*	*100*
E_{mc} (ksi)	460	410	360	310
σ_{my} (ksi)	10.5	10.0	8.5	6.5

iii) Polyester glass fiber pultrusion (9)

Speed (mm/min.)	*Pultrusion*	
	Strength (GPa)	*Modulus (GPa)*
0.05	0.45	19.3
0.5	0.47	19.5
5.0	0.53	20.2
50.0	0.52	26.2

TABLE VIII Equations for the study of strain rate and temperature effect

i) Fiber failure mode (Eq. (3))

$$\sigma_{1u}(T_1, \dot{\varepsilon}) = K\sigma_{fu,1}(T_1, \dot{\varepsilon})(V_f + V_m E_m(T_1, \dot{\varepsilon})/E_f(T_1, \dot{\varepsilon}))$$
$$\sigma_{1u}(T_2, \dot{\varepsilon}) = K\sigma_{fu,2}(T_2, \dot{\varepsilon})(V_f + V_m E_m(T_2, \dot{\varepsilon})/E_f(T_2, \dot{\varepsilon}))$$

ii) Fiber buckling and matrix yielding mode Eq. (6)

$$\sigma_{1u}(T_1, \dot{\varepsilon}) = K_2(V_f + V_m E_m(T_1, \dot{\varepsilon})/E_f(T_1, \dot{\varepsilon}))\sigma_{my}(T_1, \dot{\varepsilon})$$
$$\sigma_{1u}(T_2, \dot{\varepsilon}) = K_2(V_f + V_m E_m(T_2, \dot{\varepsilon})/E_f(T_2, \dot{\varepsilon}))\sigma_{my}(T_2, \dot{\varepsilon})$$

iii) Interface and matrix tensile failure mode Eq. (8)

$$\sigma_{1u}(T_1, \dot{\varepsilon}) = K_3(\pi\sigma_{a1}(T_1, \dot{\varepsilon}) + (\sqrt{P_f}/V_f - 2)\sigma_{mtu,1}(T_1, \dot{\varepsilon})(V_f + V_m E_m(T_1, \dot{\varepsilon})/E_f(T_1, \dot{\varepsilon}))$$
$$\sigma_{1u}(T_2, \dot{\varepsilon}) = K_3(\pi\sigma_{a2}(T_2, \dot{\varepsilon}) + (\sqrt{P_f}/V_f - 2)\sigma_{mtu,2}(T_2, \dot{\varepsilon})(V_f + V_m E_m(T_2, \dot{\varepsilon})/E_f(T_2, \dot{\varepsilon}))$$

We can use the previous equations for the studies of these effects by expressing the equations as functions of temperature and strain rate as shown in Table VIII.

From the equation in Table VIII, we see that by measuring the compressive strength at two different temperatures or strain rates, we could eliminiate the uncertainty factor K, so that changes of σ_{fu}, σ_a can be isolated and quantified.

IV. CONCLUSIONS

As stated above we found Piggott's theoretical and experimental work more advanced and realistic than that of other workers in this field. We, therefore, used his theory and expanded or modified his approaches where the revisions were required and obvious. The derived expressions were used to outline a comprehensive experiment plan to test the revised theory, derive guidelines to optimize the compressive strength of Spectra-900 composites and develop background for further refinements in theory.

References

[1] Rosen, B. W. (1965). Mechanics of Composite Strengthening, *Fiber Composite Materials*, Chap. 3, ASM, Metals Park, OH.

[2] Hayashi, T. and Koyama, K. Proceedings of the 5th International Conference on the Mechanical Behavior of Materials, August 1971, p. 104.

[3] Wilde, P. and Piggott, M. R. (1980). *J. Mater. Sci.*, **15**, 2811.
[4] DeFerran, E. M. and Harris, B. (1970). *J. Comp. Mater.*, **4**, 62.
[5] Hancox, N. L. (1975). *J. Mater. Sci.*, **10**, 234.
[6] Piggott, M. R. and Harris, B. (1980). *J. Mater. Sci.*, **15**, 2523.
[7] Davis, J. G. (1975). ASTM STP 580, 364.
[8] Martinez, G. M., Piggott, M. R., Bainbridge, D. M. R. and Harris, B. (1981). *J. Mater. Sci.*, **16**, 2831.
[9] Developments in Reinforced Plastics – 4, Pritchard, G. Ed., Elsevier Applied Science Publishers, London and New York, Chap. **4**, 1984.
[10] Piggott, M. R. (1981). *J. Mater. Sci.*, **16**, 2837.
[11] Chaplin, C. R. (1977). *J. Mater. Sci.*, **12**, 347.
[12] Swift, D. G. (1975). *J. Phys. D.*, **8**, 223.
[13] Ewins, P. D. and Potter, T. T. (1980). *Phil. Trans. Roy. Soc.*, (London), A 294, 507.
[14] Parry, T. V. and Wronsky, A. S. (1982). *J. Mater. Sci.*, **17**, 3656.
[15] Lamb, G. E. R., Butler, R. H. and Prevorsek, D. C. *Textile Res. J.*, March 1975, p. 267.
[16] Van Krevelen, D. W. and Hoftyzer, P. J. (1976). Properties of Polymers – their estimation and correlation with chemical structure-, Elsevier Scientific Publishing Co.
[17] Plastics, desk-top-data-bank, 5th Ed., the International Plastics Selector, Inc., 1980.
[18] CRC Handbook of Materials Science, **2**, Section 4, Ed. by Charles, T. Lynch CRC Press Inc.
[19] Epon Resin Structural Reference Manual, Shell Chemical Co.
[20] Dow Epoxy Resins, Products Literature, DER Flexible Epoxy Resins.
[21] Ciba-Geigy epoxy resins and hardeners general catalog.
[22] Handbook of Composites, Ed. by Lubin G. Van Nostrand Pub. Co. 1982.
[23] Hull, D. (1981). An Introduction to Composite Materials, Cambridge Solid State Science Series.